nature nanotechnology

LETTERS

https://doi.org/10.1038/s41565-021-00927-y

Check for updates

Continuous-wave near-infrared stimulated-emission depletion microscopy using downshifting lanthanide nanoparticles

Liangliang Liang[1,8], Ziwei Feng[2,8], Qiming Zhang[3,8], Thang Do Cong[4], Yu Wang[5], Xian Qin[1], Zhigao Yi[1], Melgious Jin Yan Ang[1], Lei Zhou[1], Han Feng[6], Bengang Xing[4], Min Gu[3] ✉, Xiangping Li[2] ✉ and Xiaogang Liu[1,5,7] ✉

Stimulated-emission depletion (STED) microscopy has profoundly extended our horizons to the subcellular level[1–3]. However, it remains challenging to perform hours-long, autofluorescence-free super-resolution imaging in near-infrared (NIR) optical windows under facile continuous-wave laser depletion at low power[4,5]. Here we report downshifting lanthanide nanoparticles that enable background-suppressed STED imaging in all-NIR spectral bands ($\lambda_{excitation}$ = 808 nm, $\lambda_{depletion}$ = 1,064 nm and $\lambda_{emission}$ = 850–900 nm), with a lateral resolution of below 20 nm and zero photobleaching. With a quasi-four-level configuration and long-lived (τ > 100 µs) metastable states, these nanoparticles support near-unity (98.8%) luminescence suppression under 19 kW cm^{-2} saturation intensity. The all-NIR regime enables high-contrast deep-tissue (~50 µm) imaging with approximately 70 nm spatial resolution. These lanthanide nanoprobes promise to expand the application realm of STED microscopy and pave the way towards high-resolution time-lapse investigations of cellular processes at superior spatial and temporal dimensions.

Organic fluorophores are commonly used for STED microscopy and other super-resolution imaging techniques[6–12]. However, synchronized intense pulses in STED microscopy are often employed to compete with fast spontaneous fluorescence kinetics ($k > 10^8$ s^{-1})[5,13], resulting in potential phototoxicity, photobleaching and a significant depletion-induced re-excitation (DIRE) background. Moreover, organic fluorophores often work in the visible-light region, which reduces their applicability in deep tissues[14]. Although spin-forbidden transitions significantly reduce the emission rates ($k < 10^6$ s^{-1}), triplet-to-singlet transitions usually luminesce in low-temperature, anoxic environments[15]. Laporte's parity-selection rule implies that electric-dipole 4*f*–4*f* transitions in lanthanide ions are forbidden. However, when the lanthanide ion experiences non-centrosymmetric interactions, the admixture of opposite parity into 4*f* wavefunctions can relax the selection rule and produce long-lived luminescence[16–19]. With drastically stabilized emitting states (τ > 100 µs), lanthanide emitters have been explored for ultraviolet-visible-NIR lasing[20–22] and, very recently, photon-avalanching-based super-resolution imaging[23]. Furthermore, for emitters with a quasi-four-level energy configuration, the lower-lying level is well above the ground state; thus, significant population inversion can be sustained by low-power pumping, and re-absorption of laser radiation in a gain medium can be avoided completely. For example, neodymium (Nd), featuring efficient stimulated emission, can be used to generate NIR lasing even under solar-light pumping[24]. By principles similar to lasing, we believe that STED microscopy employing rationally engineered lanthanide emitters can circumvent the aforementioned fundamental constraints and enable long-term background-suppressed super-resolution imaging with low-power continuous-wave (CW) lasers in the NIR optical window (Fig. 1a).

To validate our hypothesis, neodymium emitters were randomly integrated within hexagonal-phase $NaYF_4$ nanocrystals with a large deviation from inversion symmetry (Supplementary Fig. 1)[25]. The opposite-parity-state admixing nature in neodymium emitters was confirmed by density functional theory calculations (Supplementary Fig. 2). When excited at 808 nm (NIR-I), these neodymium-activated nanocrystals containing hundreds of slow-emitting emitters produce two intense downshifted luminescence bands, one centred at 864 nm (NIR-I, $^4F_{3/2} \rightarrow {}^4I_{9/2}$) and the other at 1,064 nm (NIR-II, $^4F_{3/2} \rightarrow {}^4I_{11/2}$; Fig. 1b and Supplementary Fig. 3). The 864 nm emission band was suppressed almost completely by adding a CW 1,064 nm depletion beam (Fig. 1c). Upon 808 nm excitation, the optimal sample with 1% neodymium activators achieved an absolute quantum yield of ~27.6% (Fig. 2a). Moreover, the downshifting luminescence at 864 nm from the $NaYF_4$:Nd (1%) nanocrystals was nearly four orders of magnitude brighter than its upconverting luminescence at 588 nm (Supplementary Fig. 4). The intense downshifting luminescence can be ascribed to efficient population accumulation at the $^4F_{3/2}$ level, since closely spaced high-energy levels suffer rapid non-radiative relaxation to the metastable state ($^4F_{3/2}$).

Next, we investigated the STED features of the as-prepared neodymium STED nanoprobes (Supplementary Fig. 5). The intense NIR luminescence of all nanoprobes with various neodymium doping concentrations (from 0.1 to 8%) was drastically suppressed

[1]Department of Chemistry, National University of Singapore, Singapore, Singapore. [2]Guangdong Provincial Key Laboratory of Optical Fiber Sensing and Communications, Institute of Photonics Technology, Jinan University, Guangzhou, China. [3]Centre for Artificial-Intelligence Nanophotonics, School of Optical-Electrical and Computer Engineering, University of Shanghai for Science and Technology, Shanghai, China. [4]Division of Chemistry and Biological Chemistry, School of Physical & Mathematical Sciences, Nanyang Technological University, Singapore, Singapore. [5]SZU-NUS Collaborative Innovation Center for Optoelectronic Science & Technology, Institute of Microscale Optoelectronics, Shenzhen University, Shenzhen, China. [6]Nanyang Environment and Water Research Institute, Interdisciplinary Graduate Programme, Nanyang Technological University, Singapore, Singapore. [7]Joint School of National University of Singapore and Tianjin University, International Campus of Tianjin University, Fuzhou, China. [8]These authors contributed equally: Liangliang Liang, Ziwei Feng, Qiming Zhang. ✉e-mail: gumin@usst.edu.cn; xiangpingli@jnu.edu.cn; chmlx@nus.edu.sg

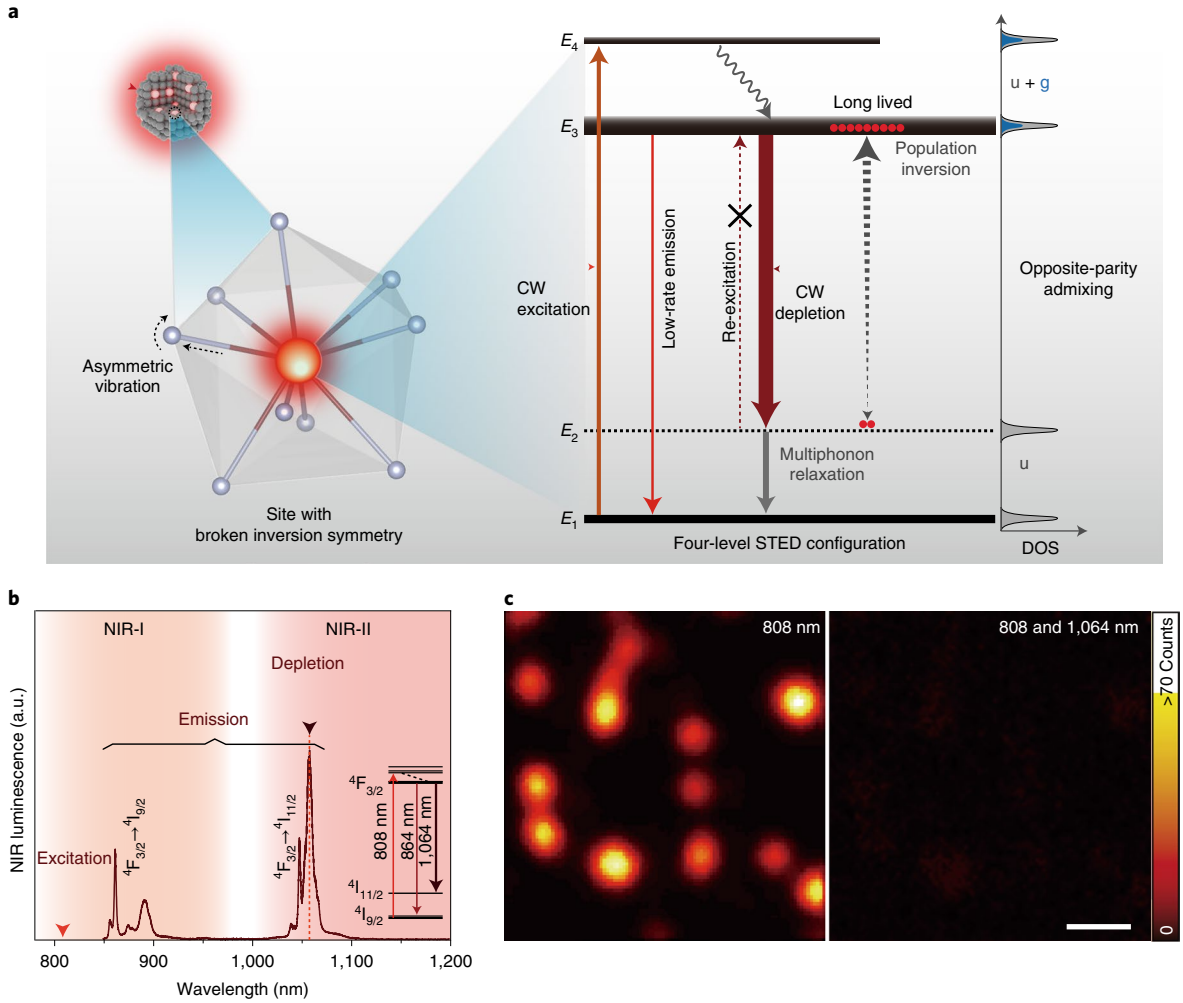

Fig. 1 | All-NIR quasi-four-level CW STED microscopy. a, Working principle of the low-rate quasi-four-level system mediated by parity-forbidden transitions for efficient STED. The parity-selection rule of the emitters is partially relaxed at a lattice site without inversion symmetry, showing slow forced-subshell electronic transitions. A significant population inversion builds up between the long-lived metastable level (E_3) and the fast-evacuated bottom level (E_2) of the quasi-four-level system, enabling efficient STED of E_3, which largely mitigates the luminescence. The terms 'u' (marked in grey) and 'g' (marked in blue) represent the ungerade and gerade parity involved in the transitions, respectively, and 'u + g' illustrates the possible opposite-parity-state admixing. DOS, density of states. **b**, Downshifted luminescence spectrum of neodymium-doped sodium yttrium fluoride ($NaYF_4$:Nd) nanoprobes under a xenon lamp (~808 nm, 5 mW cm^{-2}). The inset shows the corresponding downshifting luminescence pathway. **c**, NIR luminescence-mediated confocal images of $NaYF_4$:Nd (1%) nanoprobes under 808 nm illumination (left) and 808 nm/1,064 nm co-illumination (right). The 864 nm emission band was extracted for detection. Pixel dwell time, 100 µs. Scale bar, 1 µm. The experiment was repeated three times independently with similar results.

upon depletion with a CW 1,064 nm beam. The DIRE background inherent to conventional STED nanoprobes was undetectable (Fig. 2b). Notably, slight doping with neodymium emitters facilitated the depletion processes in the nanoprobes, as indicated by the L-shaped depletion curves. Reducing the emitter concentration from 8 to 0.1% enhanced the luminescence depletion efficiency (η) of the nanoprobes from 91 to 98.2% and diminished the saturation intensity (I_{sat}) by one order of magnitude (to ~0.045 MW cm^{-2}; Fig. 2c). Moreover, when the excitation power was reduced (Fig. 2d), the depletion efficiency was promoted to 98.8% at ~19 kW cm^{-2} saturation intensity, which is almost ten times lower than that (0.19 MW cm^{-2}) reported in a previous study involving photon upconversion[26] and is over two orders of magnitude lower than that of an organic dye[5] (3.3 MW cm^{-2}) or nitrogen-vacancy centres[27] (6.6 MW cm^{-2}). Besides, it should be noted that the minimum diffusion and high photostability of the nanoprobes can also contribute to the high depletion efficiency[27,28]. By contrast, conventional organic-dye-mediated STED microscopy is generally limited to a maximum depletion efficiency of ~90% (refs. [5,29,30]).

The superior STED performance of the neodymium STED nanoprobes is mainly attributable to their unique four-level configuration, which involves parity-conserved *f*–*f* transitions (Fig. 3a). Owing to the partially forbidden *f*–*f* transitions, the metastable-level (E_3, $^4F_{3/2}$) lifetimes of all the prepared neodymium STED nanoprobes were longer than 50 µs (Fig. 3b). For nanoprobes with a low neodymium content, as the increased average emitter distance (from approximately 1 to 4 nm) diminishes cross-relaxation (Supplementary Fig. 6), the lifetime of the NIR luminescence can be further prolonged to 400 µs, over four orders of magnitude longer than that of organic dyes or quantum dots (typically shorter than 10 ns). As corroborated by simulation, a long-lived metastable level (>10 µs) guarantees strong population inversion in a quasi-four-level energy-state model (Supplementary Fig. 7)[31]. Moreover, unlike conventional four-level fluorescence systems with

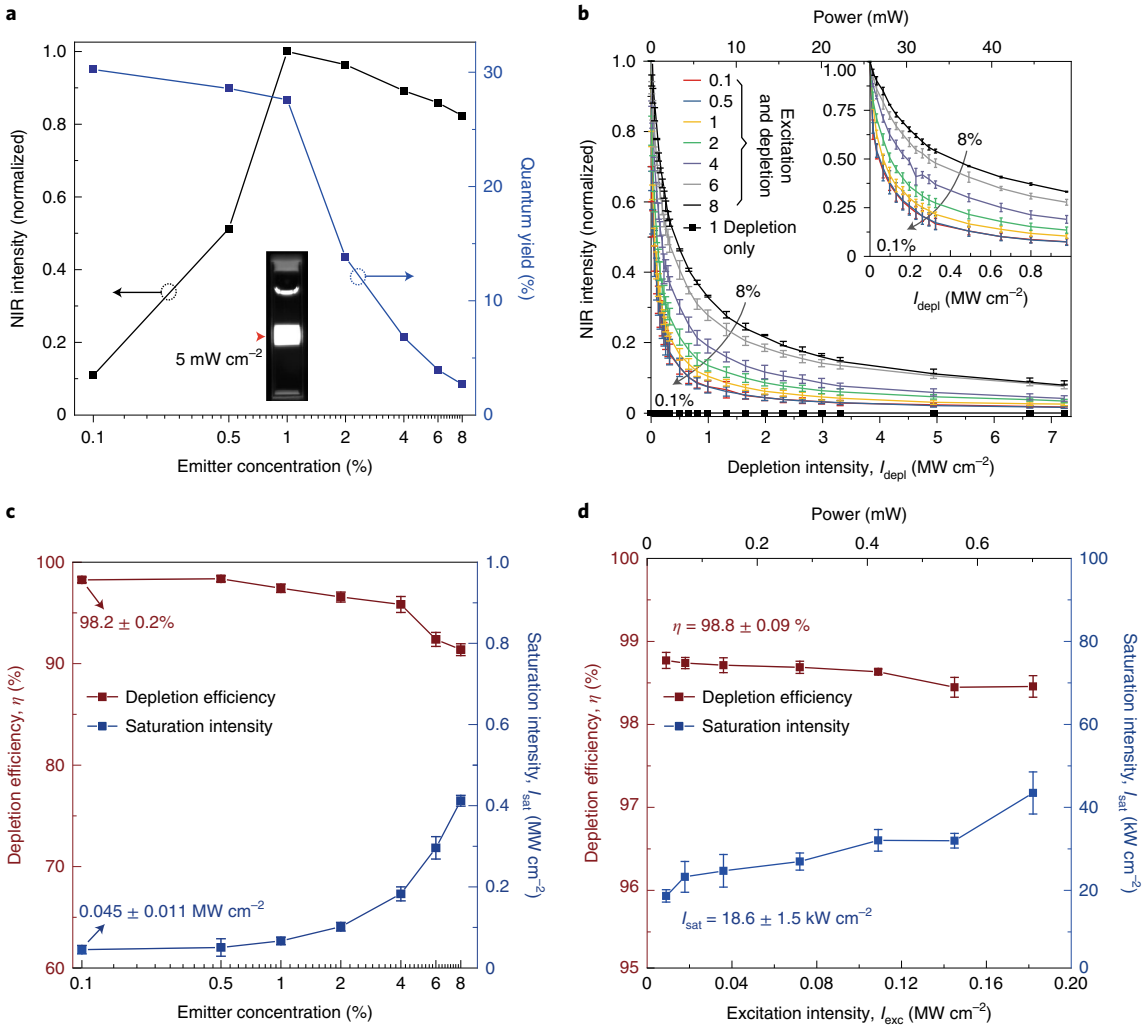

Fig. 2 | Optical switching features of neodymium-activated NIR STED nanoprobes. a, Downshifting luminescence intensities and corresponding absolute quantum yield of neodymium STED nanoprobes versus the emitter doping concentration (0.1–8 mol%). The inset shows a photograph of $NaYF_4$:Nd (1%) nanocrystals dispersed in cyclohexane under 808 nm xenon lamp excitation at 5 mW cm^{-2}. **b**, NIR luminescence suppression features of $NaYF_4$:Nd (*x*%, *x* = 0.1, 0.5, 1, 2, 4, 6 and 8) STED nanoprobes upon co-illumination with a CW 808 nm excitation beam (0.3 MW cm^{-2}) and a CW 1,064 nm depletion beam, where the closed square symbols indicate the depletion beam only. The inset is an enlarged view of the low depletion intensity range. **c**, Saturation intensity (I_{sat}) and corresponding depletion efficiency (η) versus emitter concentration in the STED nanoprobes. **d**, Saturation intensity and depletion efficiency of the neodymium (0.1%) STED nanoprobe versus excitation power (I_{exc}) at 808 nm. Error bars in **b**–**d** are ±1 s.d. of $n = 3$ independent measurements, and data are presented as mean values.

a thermally reachable level (E_2), neodymium activators feature a substantial energy barrier (~2,100 cm^{-1}) between the ground level (E_1) and E_2. As such, the thermal population of E_2 from E_1 is exceptionally inefficient, as evidenced by the temperature-dependent absorption spectra (Fig. 3c)[32]. As the temperature is increased, the population redistributed in the sub-levels of E_1, and the absorbance gradually declined. Nevertheless, no absorption stemming from the $E_2 \rightarrow E_3$ transition can be observed even at 373 K, signifying that E_2 is quasi-empty and imparts negligible DIRE to E_3. Moreover, as indicated by simulation results (Supplementary Fig. 8), rapid relaxation to E_1 promptly evacuated the population accumulated on E_2, further strengthening the quasi-empty nature of E_2 and mitigating DIRE. Owing to the significant population inversion and the long-lived metastable level (E_3, $^4F_{3/2}$) of the neodymium emitters, their slow luminescence kinetics (<10^4 s^{-1}) can be readily suppressed by the depletion beam, resulting in a near-unity depletion efficiency and negligible background noise. As revealed in experimental and simulated results (Fig. 3d and Supplementary Fig. 9), the NIR luminescence lifetime ($^4F_{3/2}$ level) declined sharply from 292 µs to below 25 µs under a depletion intensity of 0.5 MW cm^{-2}. After increasing the depletion power to 5 MW cm^{-2}, the lifetime was further reduced to 8.5 µs, indicating that the STED process contributed 97.1% of the overall depopulation process of the metastable level.

Near-unity luminescence depletion is critical for achieving high-resolution STED imaging because the maximum suppression of luminescence can eliminate background noise and improve signal-to-noise ratios. Neodymium-activated nanoparticles are highly resistant to surface quenching. Surface passivation with an optically inert sodium gadolinium fluoride ($NaGdF_4$) layer does not markedly affect the luminescence of the nanoparticles (Supplementary Fig. 10). This property circumvents the tradeoff between the high brightness and small physical dimensions of the lanthanide nanoprobes. Small nanoprobes are ideal for high-efficiency cell labelling. We prepared monodisperse $NaGdF_4$:Nd (1%) nanoprobes (6.68 ± 0.8 nm diameter) on glass slides for STED imaging (Fig. 4a). Under laser scanning at 808 nm, a

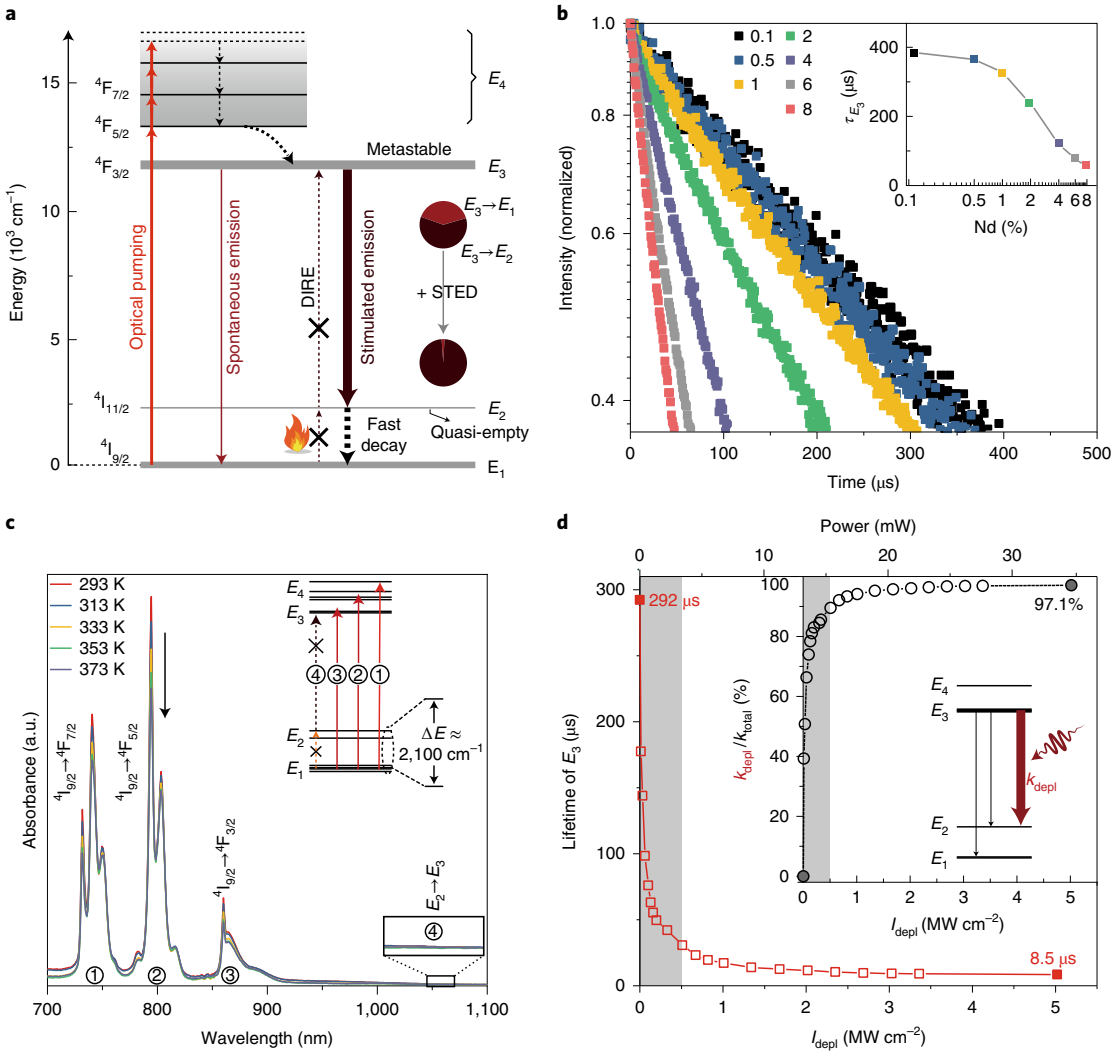

Fig. 3 | Mechanistic investigation of the neodymium-activated nanocrystals for superior STED. a, Proposed optical emission depletion mechanism of the NIR downshifting luminescence in the neodymium-mediated STED nanoprobes. **b**, Metastable-level lifetimes of neodymium STED nanoprobes with different neodymium doping concentrations (0.1–8%). The inset shows the fitted luminescence lifetime (τ_{E_3}) values. **c**, Temperature-dependent (293–373 K) absorption spectra of the prepared nanoprobes (40% Nd) dispersed in glycerol. The inset shows the absorption transitions in the neodymium emitters. **d**, NIR luminescence lifetime variation of neodymium (1%) STED nanoprobes versus the applied CW depletion power. The inset plots the contribution from the STED to the overall depopulation processes of the metastable level as a function of the depletion power (note the sharp increase at low power).

diffraction-limited resolution of ~460 nm was measured. This value was readily sharpened to ~80 nm when a 1,064 nm doughnut beam (0.5 MW cm^{-2}) was applied. In addition, in a line-profile analysis of a selected area containing single nanoparticles, the lateral resolution even reached below 20 nm (19.32 nm, I_{depl} = 7.1 MW cm^{-2}, ~140 mW in average power), a 24-fold improvement over the optical diffraction barrier, or 1/42 of the excitation wavelength (Fig. 4b–d). These nanoprobes showed no sign of photobleaching after two hours of irradiation (Fig. 4e). Although fluorescent nanodiamonds with nitrogen-vacancy centres also present remarkable photostability, they require harsh synthesis conditions, have a broad size distribution and a much higher saturation intensity[33,34]. Furthermore, as $NaGdF_4$:Nd nanocrystals offer facile hydrophobic-to-hydrophilic surface modification and negligible cytotoxicity (Supplementary Fig. 11a–c), we next implemented STED imaging on immunostained HeLa cells with microtubules labelled with antibody-conjugated neodymium STED nanoprobes (Fig. 4f–h and Supplementary Fig. 11d). As shown in the line-profile analysis, the intracellular microtubule structures were visualized down to a resolution of 57 nm.

For STED microscopy in the visible region, short-wavelength photons usually lead to phototoxicity and their working depth in tissue is strongly limited by light attenuation and aberration. For neodymium STED nanoprobes, with all wavelengths (λ_{exc} = 808 nm, λ_{em} = 850–900 nm and λ_{depl} = 1,064 nm) confined in the NIR window, the phototoxicity could be efficiently eliminated. To demonstrate the deep-tissue super-resolution imaging capability, these nanoprobes were first dispersed on glass slides, and mouse-brain slices of various thicknesses (5–50 μm) were then placed onto the nanoprobe-modified slides. These nanoprobes achieved a relatively consistent resolution of ~70 nm deep within the brain tissues without needing aberration correction (Fig. 4i,j and Supplementary Fig. 12). The high resolution of the neodymium STED nanoprobes in deep tissues was attributed to two factors: the high signal-to-noise ratio induced by the largely mitigated light attenuation and the reduced chromatic aberration due to a subtle refractive-index difference between the NIR light beams[35,36].

In conclusion, our quasi-four-level neodymium-activated downshifting nanoprobes have achieved near-unity (>98%)

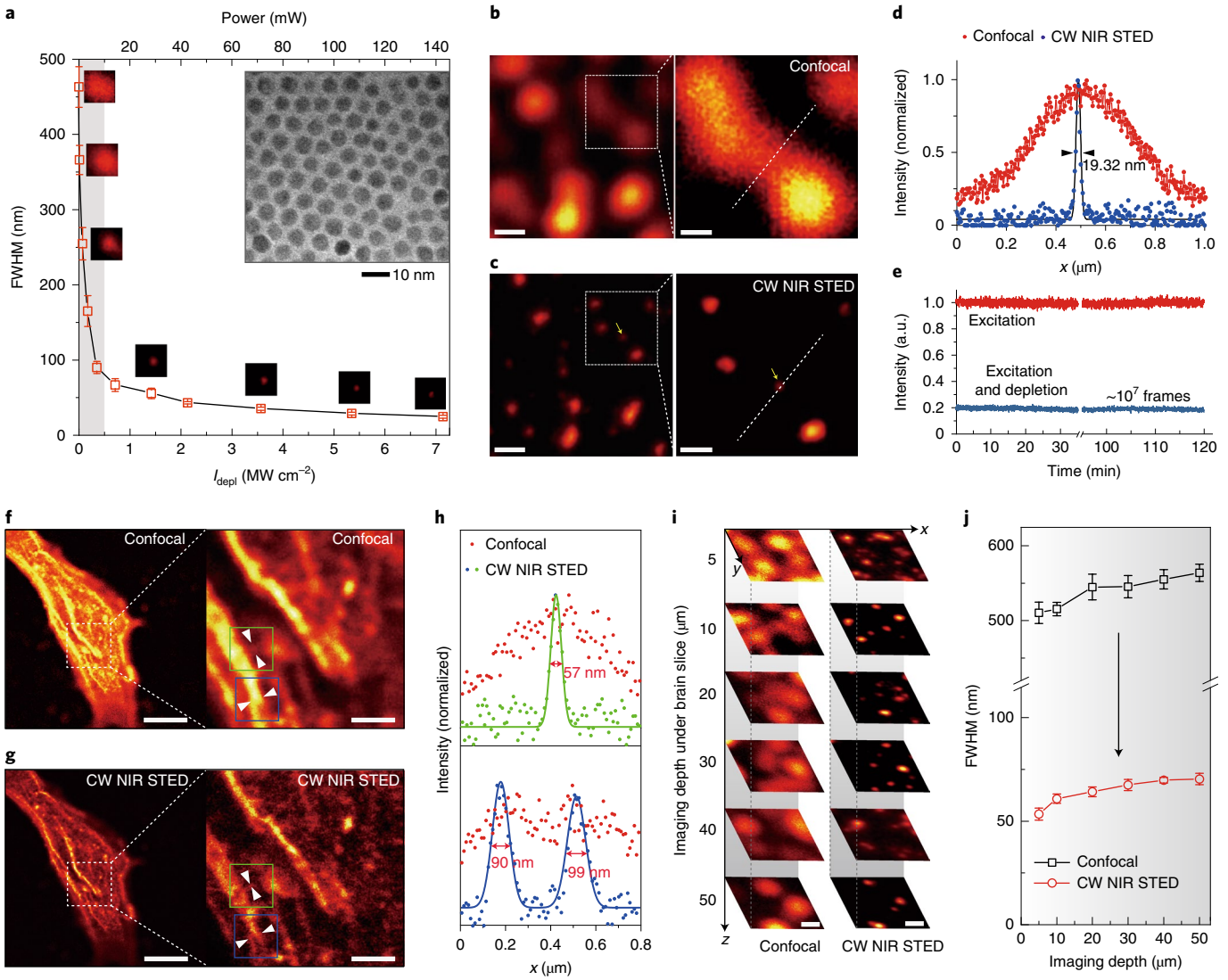

Fig. 4 | Low-power full-NIR CW STED imaging of subcellular structures and deep-tissue super-resolution imaging. a, Measured lateral resolution enhancement versus depletion power. The CW 808 nm excitation was maintained at 0.1 MW cm^{-2}. Pixel dwell time, 100 μs. Error bars, ±1 s.d. of $n = 3$ independent measurements. FWHM, full-width at half-maximum. The inset shows the TEM image of $NaGdF_4$:Nd (1%) nanoprobes producing the shown super-resolution data. **b**,**c**, Confocal (**b**) and super-resolution (**c**) images of $NaGdF_4$:Nd (1%) nanoprobes. The excitation and depletion intensities were 0.1 and 7.1 MW cm^{-2}, respectively. The regions enclosed by the dashed boxes are magnified in the corresponding right panels. Left scale bars, 500 nm; right scale bars, 200 nm. Pixel dwell time, 100 μs. The experiments in **b** and **c** were repeated three times independently with similar results. **d**, Normalized intensity profiles along the dashed lines crossing a single nanoparticle in **b** and **c**. **e**, Time recording of NIR luminescence intensity under 808 nm excitation and 808/1,064 nm co-irradiation on a single spot for two hours. **f**,**g**, Standard (**f**) and super-resolution mode (**g**) imaging of Hela cells stained with neodymium STED nanoprobes. Left scale bars, 10 μm (original images); right scale bars, 2 μm (enlarged images). The experiments in **f** and **g** were repeated three times independently with similar results. **h**, Intensity profile analysis of selected areas from **f** and **g**. **i**, Imaging comparison between the standard confocal and super-resolution modes using the developed nanoprobes at different depths beneath mouse-brain slices. Scale bars, 500 nm. **j**, The corresponding FWHM from **i**. Error bars in **j** are defined as ±1 s.d. of $n = 3$ independent measurements, and data are presented as mean values.

depletion with a saturation intensity of ~19 kW cm^{-2}. The slow parity-forbidden transitions of the quasi-four-level neodymium emitters enable a stable emitting state with significant population inversion without a thermally coupled re-excitation background, mitigating the fundamental constraints of low depletion efficiency, low imaging depth and high saturation intensity. This class of nanoprobes is not limited to nanoparticles activated with lanthanide ions, but can be extended through rational ligand-/crystal-field engineering. For instance, numerous transition metals can be integrated into nanoscale frameworks such as nanocrystals, organometallic complexes and metal–organic frameworks. Further developments in luminescent nanoprobe labelling with improved bioconjugation efficiency and minimized non-specific binding are likely to enable multiplex target detection and long-term tracking of subcellular bio-events in deep tissues[37]. Meanwhile, the viability of low-power CW illumination can significantly miniaturize the size and cost of the imaging system and promote the development of compact and possibly portable STED microscopes.

Online content

Any methods, additional references, Nature Research reporting summaries, source data, extended data, supplementary information,

acknowledgements, peer review information; details of author contributions and competing interests; and statements of data and code availability are available at https://doi.org/10.1038/s41565-021-00927-y.

Received: 13 November 2020; Accepted: 5 May 2021;
Published online: 14 June 2021

References

1. Hell, S. W. Far-field optical nanoscopy. *Science* **316**, 1153–1158 (2007).
2. Hell, S. W. & Wichmann, J. Breaking the diffraction resolution limit by stimulated emission: stimulated-emission-depletion fluorescence microscopy. *Opt. Lett.* **19**, 780–782 (1994).
3. Vicidomini, G. et al. Sharper low-power STED nanoscopy by time gating. *Nat. Methods* **8**, 571–573 (2011).
4. Klar, T. A., Jakobs, S., Dyba, M., Egner, A. & Hell, S. W. Fluorescence microscopy with diffraction resolution barrier broken by stimulated emission. *Proc. Natl Acad. Sci. USA* **97**, 8206–8210 (2000).
5. Willig, K. I., Harke, B., Medda, R. & Hell, S. W. STED microscopy with continuous wave beams. *Nat. Methods* **4**, 915–918 (2007).
6. Chen, B.-C. et al. Lattice light-sheet microscopy: imaging molecules to embryos at high spatiotemporal resolution. *Science* **346**, 1257998 (2014).
7. Bates, M., Huang, B., Dempsey, G. T. & Zhuang, X. Multicolor super-resolution imaging with photo-switchable fluorescent probes. *Science* **317**, 1749–1753 (2007).
8. Betzig, E. et al. Imaging intracellular fluorescent proteins at nanometer resolution. *Science* **313**, 1642–1645 (2006).
9. Fölling, J. et al. Fluorescence nanoscopy by ground-state depletion and single-molecule return. *Nat. Methods* **5**, 943–945 (2008).
10. Gwosch, K. C. et al. MINFLUX nanoscopy delivers 3D multicolor nanometer resolution in cells. *Nat. Methods* **17**, 217–224 (2020).
11. Klar, T. A. & Hell, S. W. Subdiffraction resolution in far-field fluorescence microscopy. *Opt. Lett.* **24**, 954–956 (1999).
12. Eggeling, C. et al. Direct observation of the nanoscale dynamics of membrane lipids in a living cell. *Nature* **457**, 1159–1162 (2008).
13. Vicidomini, G., Bianchini, P. & Diaspro, A. STED super-resolved microscopy. *Nat. Methods* **15**, 173–182 (2018).
14. Hoebe, R. et al. Controlled light-exposure microscopy reduces photobleaching and phototoxicity in fluorescence live-cell imaging. *Nat. Biotechnol.* **25**, 249–253 (2007).
15. An, Z. et al. Stabilizing triplet excited states for ultralong organic phosphorescence. *Nat. Mater.* **14**, 685–690 (2015).
16. Bünzli, J.-C. G., Chauvin, A.-S., Kim, H. K., Deiters, E. & Eliseeva, S. V. Lanthanide luminescence efficiency in eight-and nine-coordinate complexes: role of the radiative lifetime. *Coord. Chem. Rev.* **254**, 2623–2633 (2010).
17. Malta, O. Mechanisms of non-radiative energy transfer involving lanthanide ions revisited. *J. Non Cryst. Solids* **354**, 4770–4776 (2008).
18. O'Brien, J. J. & O'Brien, J. F. The Laporte selection rule in electronic absorption spectroscopy. *J. Coll. Sci. Teach.* **29**, 138–140 (1999).
19. Wisser, M. D. et al. Strain-induced modification of optical selection rules in lanthanide-based upconverting nanoparticles. *Nano Lett.* **15**, 1891–1897 (2015).
20. Jackson, S. D. Towards high-power mid-infrared emission from a fibre laser. *Nat. Photonics* **6**, 423–431 (2012).
21. Fernandez-Bravo, A. et al. Continuous-wave upconverting nanoparticle microlasers. *Nat. Nanotechnol.* **13**, 572–577 (2018).
22. Chen, X. et al. Confining energy migration in upconversion nanoparticles towards deep ultraviolet lasing. *Nat. Commun.* **7**, 10304 (2016).
23. Lee, C. et al. Giant nonlinear optical responses from photon-avalanching nanoparticles. *Nature* **589**, 230–235 (2021).
24. Lando, M., Kagan, J., Linyekin, B. & Dobrusin, V. A solar-pumped Nd:YAG laser in the high collection efficiency regime. *Opt. Commun.* **222**, 371–381 (2003).
25. Wang, F., Deng, R. & Liu, X. Preparation of core–shell $NaGdF_4$ nanoparticles doped with luminescent lanthanide ions to be used as upconversion-based probes. *Nat. Protoc.* **9**, 1634–1644 (2014).
26. Liu, Y. et al. Amplified stimulated emission in upconversion nanoparticles for super-resolution nanoscopy. *Nature* **543**, 229–233 (2017).
27. Rittweger, E., Han, K. Y., Irvine, S. E., Eggeling, C. & Hell, S. W. STED microscopy reveals crystal colour centres with nanometric resolution. *Nat. Photonics* **3**, 144–147 (2009).
28. Han, K. Y., Kim, S. K., Eggeling, C. & Hell, S. W. Metastable dark states enable ground state depletion microscopy of nitrogen vacancy centers in diamond with diffraction-unlimited resolution. *Nano Lett.* **10**, 3199–3203 (2010).
29. Hanne, J. et al. STED nanoscopy with fluorescent quantum dots. *Nat. Commun.* **6**, 7127 (2015).
30. Gao, P., Prunsche, B., Zhou, L., Nienhaus, K. & Nienhaus, G. U. Background suppression in fluorescence nanoscopy with stimulated emission double depletion. *Nat. Photonics* **11**, 163–169 (2017).
31. Koechner, W. *Solid-State Laser Engineering* 38–101 (Springer, 2006).
32. White, J. O. Parameters for quantitative comparison of two-, three-, and four-level laser media, operating wavelengths, and temperatures. *IEEE J. Quantum Electron.* **45**, 1213–1220 (2009).
33. Rehor, I. & Cigler, P. Precise estimation of HPHT nanodiamond size distribution based on transmission electron microscopy image analysis. *Diam. Relat. Mater.* **46**, 21–24 (2014).
34. Han, K. Y. et al. Three-dimensional stimulated emission depletion microscopy of nitrogen-vacancy centers in diamond using continuous-wave light. *Nano Lett.* **9**, 3323–3329 (2009).
35. Gu, Y. et al. High-sensitivity imaging of time-domain near-infrared light transducer. *Nat. Photonics* **13**, 525–531 (2019).
36. Chen, C. et al. Multi-photon near-infrared emission saturation nanoscopy using upconversion nanoparticles. *Nat. Commun.* **9**, 3290 (2018).
37. Jin, D. et al. Nanoparticles for super-resolution microscopy and single-molecule tracking. *Nat. Methods* **15**, 415–423 (2018).

Reporting Summary. Further information on research design is available in the Nature Research Reporting Summary linked to this article.

Data availability

Source data are provided with this paper. The data that support the findings of this study are available within the article and its Supplementary Information. Additional data are available from the corresponding authors upon request.

Acknowledgements

This work is supported by the National Key R&D Program of China (no. 2018YFA0902600 and no. 2018YFB1107200), the National Natural Science Foundation of China (21635002, 21771135, 21871071 and 61975123), the Ministry of Education, Singapore (MOE2017-T2-2-110), the Agency for Science, Technology and Research (A*STAR) (grant no. A1883c0011 and no. A1983c0038), National Research Foundation, the Prime Minister's Office of Singapore under its NRF Investigatorship Programme (award no. NRF-NRFI05-2019-0003), the National Basic Research Program of China (973 Program, grant no. 2015CB932200), Zhangjiang National Innovation Demonstration Zone (ZJ-2019-ZD-005) and the Guangdong Provincial Innovation and Entrepreneurship Project (grant no. 2016ZT06D081). We thank X. Zhao, J. Chen and Z. Mu for technical assistance with the TEM imaging and NIR spectral measurements. We also thank J. Hong for absorption spectra measurements.

Author contributions

L.L. and X. Liu conceived and designed the project. X. Liu, X. Li, M.G. and B.X. supervised the project and led the collaboration efforts. L.L. synthesized the nanocrystals and conducted the numerical simulations with contribution from L.Z., Q.Z. and Z.F. Optical experiments and super-resolution imaging were conducted by L.L., Z.F. and Y.W. The preparation of mouse-brain slices and cell labelling was the responsibility of Z.Y., M.J.Y.A., T.D.C. and H.F. The density functional theory calculations were conducted by X.Q. The manuscript was written by L.L., Z.F. and X. Liu. All authors participated in the discussion and analysis of the manuscript.

Competing interests

The authors declare no competing interests.

Additional information

Supplementary information The online version contains supplementary material available at https://doi.org/10.1038/s41565-021-00927-y.

Correspondence and requests for materials should be addressed to M.G., X.Li. or X.Liu.

Peer review information *Nature Nanotechnology* thanks the anonymous reviewers for their contribution to the peer review of this work.

Reprints and permissions information is available at www.nature.com/reprints.

nature research

Corresponding author(s): *Xiaogang Liu, Xiangping Li, and Min Gu*

Last updated by author(s): *2021-04-29*

Reporting Summary

Nature Research wishes to improve the reproducibility of the work that we publish. This form provides structure for consistency and transparency in reporting. For further information on Nature Research policies, see our Editorial Policies and the Editorial Policy Checklist.

Please do not complete any field with "not applicable" or n/a. Refer to the help text for what text to use if an item is not relevant to your study.
For final submission: please carefully check your responses for accuracy; you will not be able to make changes later.

Statistics

For all statistical analyses, confirm that the following items are present in the figure legend, table legend, main text, or Methods section.

n/a	Confirmed	
☐	☒	The exact sample size (*n*) for each experimental group/condition, given as a discrete number and unit of measurement
☐	☒	A statement on whether measurements were taken from distinct samples or whether the same sample was measured repeatedly
☐	☒	The statistical test(s) used AND whether they are one- or two-sided *Only common tests should be described solely by name; describe more complex techniques in the Methods section.*
☐	☒	A description of all covariates tested
☐	☒	A description of any assumptions or corrections, such as tests of normality and adjustment for multiple comparisons
☐	☒	A full description of the statistical parameters including central tendency (e.g. means) or other basic estimates (e.g. regression coefficient) AND variation (e.g. standard deviation) or associated estimates of uncertainty (e.g. confidence intervals)
☐	☒	For null hypothesis testing, the test statistic (e.g. *F*, *t*, *r*) with confidence intervals, effect sizes, degrees of freedom and *P* value noted *Give P values as exact values whenever suitable.*
☐	☒	For Bayesian analysis, information on the choice of priors and Markov chain Monte Carlo settings
☐	☒	For hierarchical and complex designs, identification of the appropriate level for tests and full reporting of outcomes
☐	☒	Estimates of effect sizes (e.g. Cohen's *d*, Pearson's *r*), indicating how they were calculated

Our web collection on statistics for biologists contains articles on many of the points above.

Software and code

Policy information about availability of computer code

Data collection	*XRD analysis software JADE. Gatan DigitalMicrograph (DM) was used as the analysis software of TEM images.*
Data analysis	*Origin and Mathematica are used for data analysis.*

For manuscripts utilizing custom algorithms or software that are central to the research but not yet described in published literature, software must be made available to editors and reviewers. We strongly encourage code deposition in a community repository (e.g. GitHub). See the Nature Research guidelines for submitting code & software for further information.

Data

Policy information about availability of data

All manuscripts must include a data availability statement. This statement should provide the following information, where applicable:

- Accession codes, unique identifiers, or web links for publicly available datasets
- A list of figures that have associated raw data
- A description of any restrictions on data availability

The data that support the findings of this study are available from the corresponding author upon reasonable request.

Field-specific reporting

Please select the one below that is the best fit for your research. If you are not sure, read the appropriate sections before making your selection.

☒ Life sciences ☐ Behavioural & social sciences ☐ Ecological, evolutionary & environmental sciences

For a reference copy of the document with all sections, see nature.com/documents/nr-reporting-summary-flat.pdf

Life sciences study design

All studies must disclose on these points even when the disclosure is negative.

Sample size	*Multiple cell samples can be found under microscope and their imaging properties can be investigated.*
Data exclusions	*No data were excluded from the analyses.*
Replication	*All attempts to repeat the experiment were successful.*
Randomization	*No data were excluded from the analyses.*
Blinding	*Data collection in different time periods.*

Behavioural & social sciences study design

All studies must disclose on these points even when the disclosure is negative.

Study description	*Briefly describe the study type including whether data are quantitative, qualitative, or mixed-methods (e.g. qualitative cross-sectional, quantitative experimental, mixed-methods case study).*
Research sample	*State the research sample (e.g. Harvard university undergraduates, villagers in rural India) and provide relevant demographic information (e.g. age, sex) and indicate whether the sample is representative. Provide a rationale for the study sample chosen. For studies involving existing datasets, please describe the dataset and source.*
Sampling strategy	*Describe the sampling procedure (e.g. random, snowball, stratified, convenience). Describe the statistical methods that were used to predetermine sample size OR if no sample-size calculation was performed, describe how sample sizes were chosen and provide a rationale for why these sample sizes are sufficient. For qualitative data, please indicate whether data saturation was considered, and what criteria were used to decide that no further sampling was needed.*
Data collection	*Provide details about the data collection procedure, including the instruments or devices used to record the data (e.g. pen and paper, computer, eye tracker, video or audio equipment) whether anyone was present besides the participant(s) and the researcher, and whether the researcher was blind to experimental condition and/or the study hypothesis during data collection.*
Timing	*Indicate the start and stop dates of data collection. If there is a gap between collection periods, state the dates for each sample cohort.*
Data exclusions	*If no data were excluded from the analyses, state so OR if data were excluded, provide the exact number of exclusions and the rationale behind them, indicating whether exclusion criteria were pre-established.*
Non-participation	*State how many participants dropped out/declined participation and the reason(s) given OR provide response rate OR state that no participants dropped out/declined participation.*
Randomization	*If participants were not allocated into experimental groups, state so OR describe how participants were allocated to groups, and if allocation was not random, describe how covariates were controlled.*

Ecological, evolutionary & environmental sciences study design

All studies must disclose on these points even when the disclosure is negative.

Study description	*Briefly describe the study. For quantitative data include treatment factors and interactions, design structure (e.g. factorial, nested, hierarchical), nature and number of experimental units and replicates.*
Research sample	*Describe the research sample (e.g. a group of tagged Passer domesticus, all Stenocereus thurberi within Organ Pipe Cactus National*

Research sample	*Monument), and provide a rationale for the sample choice. When relevant, describe the organism taxa, source, sex, age range and any manipulations. State what population the sample is meant to represent when applicable. For studies involving existing datasets, describe the data and its source.*
Sampling strategy	*Note the sampling procedure. Describe the statistical methods that were used to predetermine sample size OR if no sample-size calculation was performed, describe how sample sizes were chosen and provide a rationale for why these sample sizes are sufficient.*
Data collection	*Describe the data collection procedure, including who recorded the data and how.*
Timing and spatial scale	*Indicate the start and stop dates of data collection, noting the frequency and periodicity of sampling and providing a rationale for these choices. If there is a gap between collection periods, state the dates for each sample cohort. Specify the spatial scale from which the data are taken*
Data exclusions	*If no data were excluded from the analyses, state so OR if data were excluded, describe the exclusions and the rationale behind them, indicating whether exclusion criteria were pre-established.*
Reproducibility	*Describe the measures taken to verify the reproducibility of experimental findings. For each experiment, note whether any attempts to repeat the experiment failed OR state that all attempts to repeat the experiment were successful.*
Randomization	*Describe how samples/organisms/participants were allocated into groups. If allocation was not random, describe how covariates were controlled. If this is not relevant to your study, explain why.*
Blinding	*Describe the extent of blinding used during data acquisition and analysis. If blinding was not possible, describe why OR explain why blinding was not relevant to your study.*

Did the study involve field work? ☐ Yes ☒ No

Field work, collection and transport

Field conditions	*Describe the study conditions for field work, providing relevant parameters (e.g. temperature, rainfall).*
Location	*State the location of the sampling or experiment, providing relevant parameters (e.g. latitude and longitude, elevation, water depth).*
Access & import/export	*Describe the efforts you have made to access habitats and to collect and import/export your samples in a responsible manner and in compliance with local, national and international laws, noting any permits that were obtained (give the name of the issuing authority, the date of issue, and any identifying information).*
Disturbance	*Describe any disturbance caused by the study and how it was minimized.*

Reporting for specific materials, systems and methods

We require information from authors about some types of materials, experimental systems and methods used in many studies. Here, indicate whether each material, system or method listed is relevant to your study. If you are not sure if a list item applies to your research, read the appropriate section before selecting a response.

Materials & experimental systems

n/a	Involved in the study
☐	☒ Antibodies
☐	☒ Eukaryotic cell lines
☐	☐ Palaeontology and archaeology
☐	☐ Animals and other organisms
☐	☐ Human research participants
☐	☐ Clinical data
☐	☐ Dual use research of concern

Methods

n/a	Involved in the study
☐	☐ ChIP-seq
☐	☐ Flow cytometry
☐	☐ MRI-based neuroimaging

Antibodies

Antibodies used	*ab150077 and ab 6046 from abcam.*
Validation	*Related information can be found from the website of abcam:https://www.abcam.com/beta-tubulin-antibody-loading-control-ab6046.html and https://www.abcam.com/goat-rabbit-igg-hl-alexa-fluor-488-ab150077.html*

Eukaryotic cell lines

Policy information about cell lines

Cell line source(s)	*Fixed Hela cells are used for labeling with nanoparticles.*

Authentication	*Cell lines used were authenticated.*
Mycoplasma contamination	*Cell lines were not tested for mycoplasma contamination for nanoparticle labeling.*
Commonly misidentified lines (See ICLAC register)	*None.*

Palaeontology and Archaeology

Specimen provenance	*Provide provenance information for specimens and describe permits that were obtained for the work (including the name of the issuing authority, the date of issue, and any identifying information).*
Specimen deposition	*Indicate where the specimens have been deposited to permit free access by other researchers.*
Dating methods	*If new dates are provided, describe how they were obtained (e.g. collection, storage, sample pretreatment and measurement), where they were obtained (i.e. lab name), the calibration program and the protocol for quality assurance OR state that no new dates are provided.*

☐ Tick this box to confirm that the raw and calibrated dates are available in the paper or in Supplementary Information.

Ethics oversight	*Identify the organization(s) that approved or provided guidance on the study protocol, OR state that no ethical approval or guidance was required and explain why not.*

Note that full information on the approval of the study protocol must also be provided in the manuscript.

Animals and other organisms

Policy information about studies involving animals; ARRIVE guidelines recommended for reporting animal research

Laboratory animals	*For laboratory animals, report species, strain, sex and age OR state that the study did not involve laboratory animals.*
Wild animals	*Provide details on animals observed in or captured in the field; report species, sex and age where possible. Describe how animals were caught and transported and what happened to captive animals after the study (if killed, explain why and describe method; if released, say where and when) OR state that the study did not involve wild animals.*
Field-collected samples	*For laboratory work with field-collected samples, describe all relevant parameters such as housing, maintenance, temperature, photoperiod and end-of-experiment protocol OR state that the study did not involve samples collected from the field.*
Ethics oversight	*Identify the organization(s) that approved or provided guidance on the study protocol, OR state that no ethical approval or guidance was required and explain why not.*

Note that full information on the approval of the study protocol must also be provided in the manuscript.

Human research participants

Policy information about studies involving human research participants

Population characteristics	*Describe the covariate-relevant population characteristics of the human research participants (e.g. age, gender, genotypic information, past and current diagnosis and treatment categories). If you filled out the behavioural & social sciences study design questions and have nothing to add here, write "See above."*
Recruitment	*Describe how participants were recruited. Outline any potential self-selection bias or other biases that may be present and how these are likely to impact results.*
Ethics oversight	*Identify the organization(s) that approved the study protocol.*

Note that full information on the approval of the study protocol must also be provided in the manuscript.

Clinical data

Policy information about clinical studies

All manuscripts should comply with the ICMJE guidelines for publication of clinical research and a completed CONSORT checklist must be included with all submissions.

Clinical trial registration	*Provide the trial registration number from ClinicalTrials.gov or an equivalent agency.*
Study protocol	*Note where the full trial protocol can be accessed OR if not available, explain why.*
Data collection	*Describe the settings and locales of data collection, noting the time periods of recruitment and data collection.*
Outcomes	*Describe how you pre-defined primary and secondary outcome measures and how you assessed these measures.*

Dual use research of concern

Policy information about dual use research of concern

Hazards

Could the accidental, deliberate or reckless misuse of agents or technologies generated in the work, or the application of information presented in the manuscript, pose a threat to:

No	Yes	
☐	☐	Public health
☐	☐	National security
☐	☐	Crops and/or livestock
☐	☐	Ecosystems
☐	☐	Any other significant area

Other impacts *Describe any other significant impacts.*

Hazards *Please describe the agents/technologies/information that may pose a threat, including any agents subject to oversight for dual use research of concern.*

For examples of agents subject to oversight, see the United States Government Policy for Institutional Oversight of Life Sciences Dual Use Research of Concern.

Experiments of concern

Does the work involve any of these experiments of concern:

No	Yes	
☐	☐	Demonstrate how to render a vaccine ineffective
☐	☐	Confer resistance to therapeutically useful antibiotics or antiviral agents
☐	☐	Enhance the virulence of a pathogen or render a nonpathogen virulent
☐	☐	Increase transmissibility of a pathogen
☐	☐	Alter the host range of a pathogen
☐	☐	Enable evasion of diagnostic/detection modalities
☐	☐	Enable the weaponization of a biological agent or toxin
☐	☐	Any other potentially harmful combination of experiments and agents

Other combinations *Describe any other potentially harmful combination(s) of experiments and agents.*

Precautions and benefits

Biosecurity precautions *Describe the precautions that were taken during the design and conduct of this research, or will be required in the communication and application of the research, to minimise biosecurity risks. These may include bio-containment facilities, changes to the study design/ methodology or redaction of details from the manuscript.*

Biosecurity oversight *Describe any evaluations and oversight of biosecurity risks of this work that you have received from people or organizations outside of your immediate team.*

Benefits *Describe the benefits that application or use of this work could bring, including benefits that may mitigate risks to public health, national security, or the health of crops, livestock or the environment.*

Communication benefits *Describe whether the benefits of communicating this information outweigh the risks, and if so, how.*

ChIP-seq

Data deposition

☐ Confirm that both raw and final processed data have been deposited in a public database such as GEO.

☐ Confirm that you have deposited or provided access to graph files (e.g. BED files) for the called peaks.

Data access links
May remain private before publication. *For "Initial submission" or "Revised version" documents, provide reviewer access links. For your "Final submission" document, provide a link to the deposited data.*

Files in database submission *Provide a list of all files available in the database submission.*

Genome browser session
(e.g. UCSC)

Provide a link to an anonymized genome browser session for "Initial submission" and "Revised version" documents only, to enable peer review. Write "no longer applicable" for "Final submission" documents.

Methodology

Replicates

Describe the experimental replicates, specifying number, type and replicate agreement.

Sequencing depth

Describe the sequencing depth for each experiment, providing the total number of reads, uniquely mapped reads, length of reads and whether they were paired- or single-end.

Antibodies

Describe the antibodies used for the ChIP-seq experiments; as applicable, provide supplier name, catalog number, clone name, and lot number.

Peak calling parameters

Specify the command line program and parameters used for read mapping and peak calling, including the ChIP, control and index files used.

Data quality

Describe the methods used to ensure data quality in full detail, including how many peaks are at FDR 5% and above 5-fold enrichment.

Software

Describe the software used to collect and analyze the ChIP-seq data. For custom code that has been deposited into a community repository, provide accession details.

Flow Cytometry

Plots

Confirm that:

☐ The axis labels state the marker and fluorochrome used (e.g. CD4-FITC).

☐ The axis scales are clearly visible. Include numbers along axes only for bottom left plot of group (a 'group' is an analysis of identical markers).

☐ All plots are contour plots with outliers or pseudocolor plots.

☐ A numerical value for number of cells or percentage (with statistics) is provided.

Methodology

Sample preparation

Describe the sample preparation, detailing the biological source of the cells and any tissue processing steps used.

Instrument

Identify the instrument used for data collection, specifying make and model number.

Software

Describe the software used to collect and analyze the flow cytometry data. For custom code that has been deposited into a community repository, provide accession details.

Cell population abundance

Describe the abundance of the relevant cell populations within post-sort fractions, providing details on the purity of the samples and how it was determined.

Gating strategy

Describe the gating strategy used for all relevant experiments, specifying the preliminary FSC/SSC gates of the starting cell population, indicating where boundaries between "positive" and "negative" staining cell populations are defined.

☐ Tick this box to confirm that a figure exemplifying the gating strategy is provided in the Supplementary Information.

Magnetic resonance imaging

Experimental design

Design type

Indicate task or resting state; event-related or block design.

Design specifications

Specify the number of blocks, trials or experimental units per session and/or subject, and specify the length of each trial or block (if trials are blocked) and interval between trials.

Behavioral performance measures

State number and/or type of variables recorded (e.g. correct button press, response time) and what statistics were used to establish that the subjects were performing the task as expected (e.g. mean, range, and/or standard deviation across subjects).

Acquisition

Imaging type(s) *Specify: functional, structural, diffusion, perfusion.*

Field strength *Specify in Tesla*

Sequence & imaging parameters *Specify the pulse sequence type (gradient echo, spin echo, etc.), imaging type (EPI, spiral, etc.), field of view, matrix size, slice thickness, orientation and TE/TR/flip angle.*

Area of acquisition *State whether a whole brain scan was used OR define the area of acquisition, describing how the region was determined.*

Diffusion MRI ☐ Used ☐ Not used

Parameters *Specify # of directions, b-values, whether single shell or multi-shell, and if cardiac gating was used.*

Preprocessing

Preprocessing software *Provide detail on software version and revision number and on specific parameters (model/functions, brain extraction, segmentation, smoothing kernel size, etc.).*

Normalization *If data were normalized/standardized, describe the approach(es): specify linear or non-linear and define image types used for transformation OR indicate that data were not normalized and explain rationale for lack of normalization.*

Normalization template *Describe the template used for normalization/transformation, specifying subject space or group standardized space (e.g. original Talairach, MNI305, ICBM152) OR indicate that the data were not normalized.*

Noise and artifact removal *Describe your procedure(s) for artifact and structured noise removal, specifying motion parameters, tissue signals and physiological signals (heart rate, respiration).*

Volume censoring *Define your software and/or method and criteria for volume censoring, and state the extent of such censoring.*

Statistical modeling & inference

Model type and settings *Specify type (mass univariate, multivariate, RSA, predictive, etc.) and describe essential details of the model at the first and second levels (e.g. fixed, random or mixed effects; drift or auto-correlation).*

Effect(s) tested *Define precise effect in terms of the task or stimulus conditions instead of psychological concepts and indicate whether ANOVA or factorial designs were used.*

Specify type of analysis: ☐ Whole brain ☐ ROI-based ☐ Both

Anatomical location(s) *Describe how anatomical locations were determined (e.g. specify whether automated labeling algorithms or probabilistic atlases were used).*

Statistic type for inference (See Eklund et al. 2016) *Specify voxel-wise or cluster-wise and report all relevant parameters for cluster-wise methods.*

Correction *Describe the type of correction and how it is obtained for multiple comparisons (e.g. FWE, FDR, permutation or Monte Carlo).*

Models & analysis

n/a	Involved in the study
☐	☐ Functional and/or effective connectivity
☐	☐ Graph analysis
☐	☐ Multivariate modeling or predictive analysis

Functional and/or effective connectivity *Report the measures of dependence used and the model details (e.g. Pearson correlation, partial correlation, mutual information).*

Graph analysis *Report the dependent variable and connectivity measure, specifying weighted graph or binarized graph, subject- or group-level, and the global and/or node summaries used (e.g. clustering coefficient, efficiency, etc.).*

Multivariate modeling and predictive analysis *Specify independent variables, features extraction and dimension reduction, model, training and evaluation metrics.*